JOURNAL OF MATERIALS SCIENCE: MATERIALS IN MEDICINE **16** (2005) 101 – 106

Hydroxyapatite-coated metals: Interfacial reactions during sintering

M. WEI[1,*], A. J. RUYS[2], M. V. SWAIN[2], B. K. MILTHORPE[3], C. C. SORRELL[4]
[1]*Department of Metallurgy and Materials Engineering, University of Connecticut, CT 06269, USA*
E-mail: m.wei@ims.uconn.edu
[2]*Department of Biomedical Engineering, School of Aerospace Mechanical and Mechatronic Engineering, University of Sydney, NSW 2006, Australia*
[3]*Graduate School for Biomedical Engineering, University of New South Wales, NSW 2052, Australia*
[4]*School of Materials Science and Engineering, University of New South Wales, Sydney, NSW 2052, Australia*

Electrophoretic deposition (EPD) is a low cost flexible process for producing HA coatings on metal implants. Its main limitation is that it requires heating the coated implant in order to densify the HA. HA typically sinters at a temperature below 1150 °C, but metal implants are degraded above 1000 °C. Further, the metal induces the decomposition of the HA coating upon sintering. Recent developments have enabled EPD of metathesis-synthesised uncalcined HA which sinters at ∼ 1000 °C. The effects of temperature on HA-coated Ti, Ti6Al4V, and 316L stainless steel were investigated for dual coatings of metathesis HA sintered at 1000 °C. The use of dual HA coatings (coat, sinter, coat, sinter) enabled decomposition to be confined to the "undercoat" (HA layer 1), with the surface coating decomposition free. The tensile strength of the three metals was not significantly affected by the high sintering temperatures (925 °C $< T <$ 1000 °C). XRD/SEM/EDS analyses of the interfacial zones revealed that 316L had a negligible HA:metal interfacial zone (∼1 μm) while HA:Ti and HA:Ti6Al4V had large interfacial zones (>10 μm) comprising a TiO_2 oxidation zone and a $CaTiO_3$ reaction zone.

1. Introduction

Metals such as titanium, titanium alloy (Ti6Al4V), and 316L stainless steel have found widespread use in orthopaedic applications involving hard tissue replacement, owing to their combination of excellent mechanical properties and proven biocompatibility. However, these metals are not bioactive, i.e., they are not capable of direct bone bonding. A recently developed solution to this problem has been the development of metal implants with bioactive surface coatings. Attention has been focussed on hydroxyapatite [HA: $Ca_{10}(PO_4)_6(OH)_2$] coatings, since HA is chemically similar to bone mineral and therefore one of the few hard-tissue-replacement materials classed as bioactive, and not prone to resorption *in vivo*.

There are a number of methods reported in the literature for depositing bioactive HA coatings onto metallic implants. Of these, the most widely used is thermal spraying [1–4], which offers many benefits, but suffers from the fact that it requires complex and costly equipment, and being a line-of-sight process is unable to coat metallic implants that have complex shapes or engineered porosity for biological fixation. Processes such as sol-gel coating [5], electrochemical deposition [6], biomimetic coating [7], and electrophoretic deposition (EPD) [8] are low-cost alternatives to thermal spraying that involve deposition from a liquid medium at an ambient temperature. EPD is an attractive alternative to thermal spraying in that it is a low cost, flexible process able to produce a broad range of coating thicknesses from less than 1 μm to a few millimetres, with a high degree of control over deposit thickness. EPD is also a non-line-of-sight process, and can therefore produce uniform coatings on regular or irregular surfaces [9]. The principal limitation of EPD is that, as for many ambient-temperature powder coating processes, the deposit is in the form of a loosely held coating of particles which must be subsequently densified by heating the coated implant to elevated temperatures sufficient to sinter the HA coating. Therefore, unlike thermal spraying, densification and deposition do not occur simultaneously with EPD. HA generally must

*Author to whom all correspondence should be addressed.

be sintered at temperatures above 1150 °C to densify [2]. There are four critical issues regarding mechanical properties and phase stability of the HA coated implants during the heat-treatment:

1. Firing shrinkage of the HA
2. Thermal expansion coefficient mismatch between the HA and metal substrates
3. Thermal stability of the metal
4. Thermal stability of the HA

Firing Shrinkage. It is well known that when a ceramic densifies from the powder-compact state (typically 40–60% dense) to the dense-sintered state (typically > 90% dense), a significant amount of firing shrinkage is involved. Generally this is in the order of 15 to 20% linear shrinkage [10]. During densification, a ceramic coating is constrained by its substrate and so firing shrinkage results in severe residual tensile stresses in the coating, with the associated risk of cracking. This firing shrinkage is unavoidable in that densification of a powder deposit cannot be achieved without significant shrinkage. Partial densification will minimise shrinkage, and produce a crack-free coating, but such a poorly densified coating has insignificant bonding to the metal [11]. However, the authors have recently demonstrated that through the use of dual coatings (coat, sinter, coat, sinter) a highly densified coating can have high shrinkage and yet attain a significant bonding strength [11, 12]. This is because the "crevices" in the firing-shrinkage-cracks of the first coating are filled by the second coating, thereby resulting in a coating that undergoes significant firing shrinkage but is strongly and integrally adhered to the substrate.

Thermal Expansion Mismatch. After densification, as the coated substrate is cooled from the densification temperature, the associated temperature change of 1000 °C or more results in significant thermal contraction [13]. Therefore, in order to avoid spalling of the coating during sintering, a slow heating and cooling rate is normally required [14]. If the metal has a lower thermal expansion coefficient than the HA (α-metal < α-HA), then the coating will contract more than the metal during cooling, with the result that residual tensile stresses will be generated in the coating. Residual tensile stresses tend to induce cracking. This is the case for Ti and Ti6Al4V (α-Ti and α-Ti6Al4V are both $\sim$10.3 μm/mK; α-HA is $\sim$14 μm/mK) [11]. Alternatively, if the metal has a higher thermal expansion coefficient than the HA (α-metal>α-HA), it will contract more than the coating, causing residual compressive stresses. This is the case for 316L stainless steel (α-316L $\sim$20.5 μm/mK) [11]. Minor compressive stresses are beneficial in that they act to close cracks and therefore "toughen" the coating. Thus, a metallic substrate with a high thermal expansion coefficient is advantageous [15].

Thermal Stability of the Metal. Heating Ti to elevated temperatures causes problems with grain growth, phase changes, and oxidation. α-Ti (HCP lattice) transforms to the β-Ti phase (BCC lattice) when heated above 882 °C [16]. The addition of aluminium stabilises the α-Ti phase, and vanadium stabilises the β-Ti phase [17]. The phase transition temperature of Ti6Al4V is 1000 °C [17]. Therefore, Ti6Al4V (Ti containing 6 wt% Al and 4 wt% V) has superior elevated temperature strength. Ti and its alloys are reactive at high temperatures and oxidise easily [16]. Oxygen diffuses easily into titanium and embrittles the metal. Therefore, HA coated Ti/Ti6Al4V implants should be sintered at minimal temperatures and oxygen partial pressures (high-purity inert gas atmospheres).

316L, an austenitic stainless steel (Fe containing 17–20 wt% Cr, 12–14 wt% Ni, 2–4 wt% Mo), is a relatively low-cost material that has excellent corrosion resistance *in vivo* [18]. However, stainless steel has the advantage in that at elevated temperatures it is much less susceptible to the problems of oxidation and strength degradation than Ti or Ti6Al4V.

Thermal Stability of the HA. HA decomposes to anhydrous calcium phosphates at temperatures generally above 1300 °C [2], i.e., well above the temperatures necessary for densification. However, this decomposition temperature can be reduced significantly by the presence of adjacent non-HA phases in a HA matrix. Such phases, present as impurities in the HA [19], or as particulate or fibrous reinforcements (as previously reviewed [20]) have all been shown to reduce the decomposition temperature of the HA-matrix from the usual range of $\sim$1300–1400 °C (pure HA) down to $\sim$750 °C–1150 °C [20–22], i.e., well below the temperatures necessary for densification. This phenomenon has been studied for numerous additives which are listed in the decreasing ability to cause a phase transformation as: C, Si_3N_4, B, Al_2O_3, Ti, Y-TSZ, WC, TiC, B_4C, Stainless Steel, TiB_2, SiC, SiO_2, ZrO_2 [20–22]. Furthermore, interfacial analysis of HA-coatings on Ti6Al4V substrates heated to 950 °C [23] and 925 °C [24] has found that significant decomposition occurred in the HA coating.

Interfacial studies [25] in HA-particulate systems have suggested that the mechanism of decomposition is isomorphous substitution altering the lattice charge, resulting in expulsion of the weakly-held "OH" groups (dehydration). All additives tested have had this effect, and this probably stems from the fact that the apatite lattice is capable of extensive isomorphous substitution into the "Ca", "PO_4", and "OH" sites [26]. The actual decomposition temperature appears to depend primarily on the composition of the "impurity" phase. Previous studies with coarse metal particles in a HA matrix have found that Ti induced decomposition at $\sim$1050 °C [22] and 316L stainless steel at $\sim$950 °C [20].

Therefore, in order to fully utilise the benefits of EPD, it is necessary to minimize the HA densification temperature as much as possible. With the use of uncalcined HA, the densification temperature has been reduced to 1000 °C [2]. Recent studies have demonstrated that it is possible to produce uncalcined HA coatings by EPD [27, 28], and the authors have

found [29] that HA prepared by the metathesis process ($Ca(NO_3)_2 + (NH_4)_2HPO_4$ digested in ammonia [30]) produces the best EPD coatings compared with HA prepared by the acid-base method [31] or the calcium acetate method [32].

The purpose of the present study was to investigate the possibility that densification of EPD coatings of ultra-high-surface-area HA (metathesis HA) on Ti, Ti6Al4V, and 316L stainless steel substrates can be achieved without compromising the properties of the metal substrates nor the phase stability of the HA. To this end, the focus was on quantification of the following:

1. Tensile strength-temperature correlations for Ti, Ti6Al4V, and 316L stainless steel substrates.
2. Oxidation of the metals at the HA-metal interface.
3. Elemental diffusion across the HA-metal interface.
4. Phase composition of the coatings and interface.

2. Methods and materials

2.1. Tensile-strength-temperature correlations for metal substrates

The effects of temperature on the tensile strength of the metals was investigated in accordance with ASTM E8M-94a. Tensile testing specimens were cut from Ti, Ti6Al4V, and 316L sheets with the dimensions shown in Fig. 1. These test specimens were heat-treated at 875°, 900°, 950°, 975°, 1000°, and 1050 °C for 1 h under a flowing argon atmosphere in a resistance tube furnace. These heat-treatment protocols were identical to those used to densify the HA coatings. After heat-treatment, the dimensions of the specimens were measured. The tensile strength test was then carried out in accordance with ASTM E8M-94a using an Instron tensometer (Model 1185, Instron Ltd., High Wycombe, UK) with a cross-head speed of 2 mm/min for all tests. The tensile strength was calculated by F/A, where F was the load at failure and A was the nominal fracture area. The average and standard deviation of 5 test specimens was used for each temperature.

2.2. Electrophoretic coating

An ultra-high surface area (∼100 m^2/g) HA powder was produced in-house by the metathesis method [31] using 99.99% pure $Ca(NO_3)_2 \cdot 4H_2O$ (Ajax Chemicals) and 98% pure $(NH_4)_2HPO_4$ (Ajax Chemicals). The reaction was carried out at room temperature. The precipitates were aged in the mother liquor at room temperature for 100 days with a pH of approximately 10.

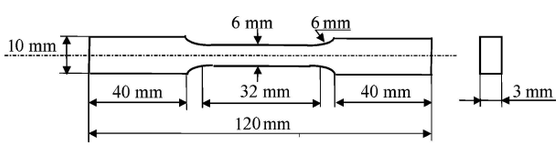

Figure 1 The shape and dimensions of the metal specimens used to determine the tensile strength of the heat-treated metals.

The HA powder was electrophoretically coated onto 18 × 36 mm Ti, Ti6Al4V, and 316L stainless steel substrates using ethanol suspensions containing 5 g/l of HA. Prior to EPD, each suspension was sonicated in an ultrasonic bath for 30 min. The metallic substrates were sandblasted with garnet, then ultrasonically washed with detergent (30 min), then washed in 95.9% acetone (15 min), and finally passivated in 25 vol% nitric acid (overnight). EPD was carried out at 50 V with deposition times of a few minutes, using 20 × 35 mm copper as anodes (the HA powder underwent cathodic deposition).

Densification of the coating took place in a resistance tube furnace under flowing high-purity argon gas, soaking for 1 h at temperatures within the range 875–1000 °C: heating rate used was 100 °C/h and the cooling rate was 50 °C/h. For each specimen, after cooling, a second coating was applied by EPD to the sintered specimen. This was followed by the same drying and sintering process, yielding a dual-coated metal substrate.

Phase analysis was conducted on the HA coatings, using x-ray diffraction (XRD: Siemens D5000). After coating 1 was heat-treated, and before coating 2 was deposited, coating 1 was examined by XRD to determine if any decomposition had occurred. Similarly, after coating 2 was deposited and heat-treated, it was also examined by XRD for decomposition of the coating. The coatings were then subjected to interfacial analysis.

Interfacial analysis involved microstructural examination of the coating cross-section by scanning electron microscopy (SEM), and quantification of elemental diffusion across the interface by energy-dispersive spectroscopy (EDS) (Hitachi S-4500 II Scanning Electron Microscope, fitted with EDS facility), via the following procedure: The metal substrates with HA dual coatings were mounted in epoxy resin. The specimens were polished parallel to the edge of the coated substrates, progressively down to a 1 μm diamond pad. They were coated with a layer of carbon (JEOL JEE-400 Vacuum Evaporator, Jeol Ltd., Japan) for SEM/EDS examination. SEM microstructural examination was carried out at 1000X involved an accelerating voltage of 20 kV. EDS analysis across the interface correlated the elemental concentrations with position: for Ti substrates, elements Ca, P, O, and Ti were examined; for Ti6Al4V substrates: elements Ca, P, O, Ti, and Al were examined; for 316L substrates, elements Ca, P, O, Fe, and Cr were examined.

Phase analysis of the interface was conducted using XRD. The dual HA coatings were removed from the substrates by gently polishing with 1200-grade SiC paper until the interface was exposed. The interface was then scanned by XRD.

3. Results and discussion

The temperature-tensile strength correlations for the three metals are shown in Fig. 2, revealing that 316L stainless steel and Ti were relatively unaffected by heat-treatment temperature below 1050 °C, and that Ti had slightly superior strength (∼600 MPa) compared with 316 L (∼500 MPa). In contrast, Ti6Al4V, which had a

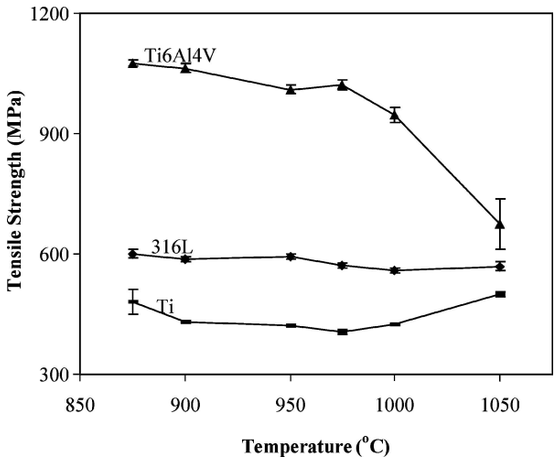

Figure 2 The effects of heat-treatment temperature on the tensile strength of the three metals: ▲; Ti6Al4V, ♦; 316L, —; Ti.

much higher strength (∼1000 MPa) than Ti or 316L, was significantly affected by the high heat-treatment temperatures, such as 1000 and 1050 °C. Its strength had dropped to the level of Ti, i.e., in the order of 600 MPa. The standard deviations of the data points (error bars) were very small, suggesting that the strength data were reliable.

These data suggest that with regard to the tensile strength of the metal implants, densifying HA-coated implants at temperatures below 1000 °C should not be a problem, and that even 1050 °C would be acceptable for all three metals unless the superior properties of Ti6Al4V were a prime concern.

The XRD analysis of the HA coatings densified at 1000 °C (the highest temperature investigated), revealed that in this "worst case scenario", HA coating 1 had a significant amount of decomposition but that decomposition was negligible in coating 2. The decomposition of HA coating 1 (undercoat) was due to the diffusion of metallic ions into the HA coating, and the diffusion of ions out of the HA lattice, thereby destabilising the HA lattice by the isomorphous substitution/charge imbalance mechanisms previously described [26, 27]. The fact that decomposition was negligible in coating 2 suggests that coating 1 acted as a diffusion barrier to decomposition in the top coating, i.e., since the first coating was already densified when the second coating was being deposited and densified, the coating 1:coating 2 interface would have been distinct (though increasingly less distinct with increasing time) as coating 2 was gradually densifying and shrinking onto coating 1.

Therefore, the dual coating approach was effective in producing decomposition-free coated surfaces, which is a critical issue in terms of subsequent *in vivo* dissolution kinetics. Interestingly, previous work by the authors has demonstrated that the dual coating approach was also important for another reason—the coating-substrate interfacial strength [12], i.e., coating 1 underwent significant firing shrinkage and the result was a high degree of cracking, then coating 2 filled in the "valleys" in the coating 1 cracks, and the result was a

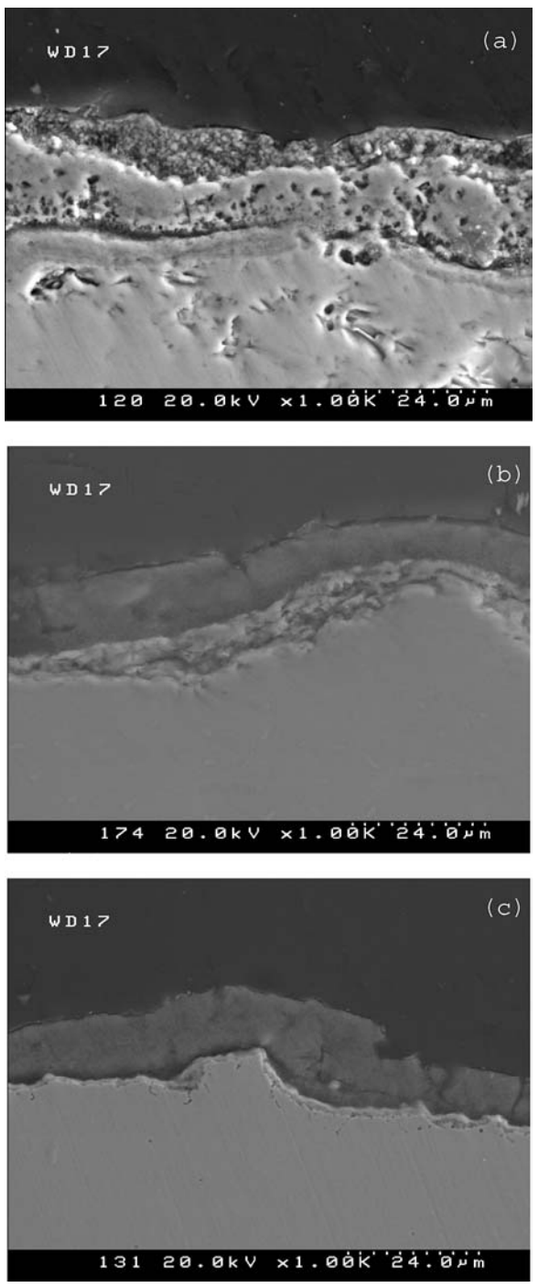

Figure 3 SEM micrograph of the HA coating on (a) Ti, (b) Ti6Al4V, and (c) 316L substrates.

significant interfacial strength (30 to 65% of the shear strength of bone) [12].

The SEM micrographs of the HA-Ti, HA-Ti6Al4V, and HA-316L specimens are shown in Fig. 3, revealing a very large interfacial region in the HA-Ti coating system (∼13 μm: slightly thicker than the HA coating), a large interfacial region in the HA-Ti6Al4V coating system (∼10 μm: slightly thinner than the coating), and a negligible interfacial region (∼1 μm) in the HA-316L coating system.

As expected, Ti was the most reactive and 316L was the least reactive at elevated temperatures. The 316L specimens had only a negligible amount of Cr_2O_3 scale at the interface. In comparison the Ti specimens had

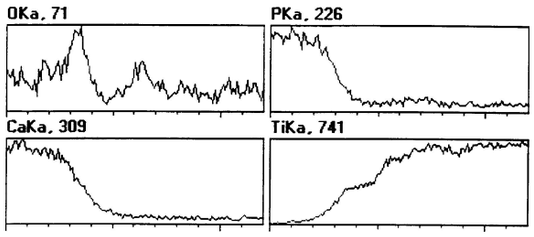

Figure 4 EDS elemental analysis across a 13.5 μm zone (1 μm divisions) of the HA-Ti interfacial zone from left (the coating surface) to right (beneath the surface of the metal) heat-treated at 950 °C for 1 h. Ca is the principal element of HA and Ti is the principal element of the substrate.

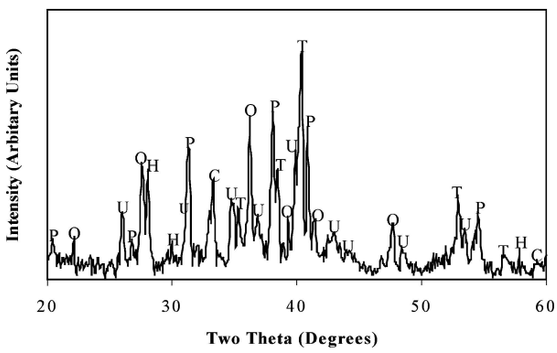

Figure 5 XRD pattern for the exposed interfacial surface (the coating was gently removed with 1200 grade SiC abrasive paper) for the HA-Ti coating system heat-treated at 1000 °C for 1 h. C = calcium titanium oxide, P = calcium phosphate, T = titanium, O = titanium oxide, H = calcium hydrogen phosphate, U = unknown.

a severe degree of interfacial reaction. The Ti6Al4V specimens were slightly less reactive since they did not contain as much of the highly reactive Ti. Therefore, all subsequent interfacial analysis focussed on the Ti specimens.

EDS elemental scans of the principal elements of the HA coating (Ca) and the Ti substrate (Ti) are presented for the most reactive interfacial system (Ti-HA) in Fig. 4. These elemental scans reveal that Ca ions had diffused towards Ti substrate at the interface, while Ti ions moved towards the HA coating. Obviously, a chemical bonding had formed at the interface.

The XRD pattern for the interfacial surface of HA and Ti substrate (after the coating was removed with 1200 grade SiC paper) is shown in Fig. 5. The XRD pattern of the HA-Ti interface revealed substantial interaction with the formation of significant amounts of calcium titanium oxide at the interface between HA coating 1 and the oxidised metal surface. It confirmed the EDS data in that it revealed a chemical activity at the HA-Ti interface.

4. Summary and conclusions

A schematic of the interface for the HA-Ti coating system was constructed from the SEM, XRD and EDS data. The schematic is shown in Fig. 6. The key features of the schematic were:

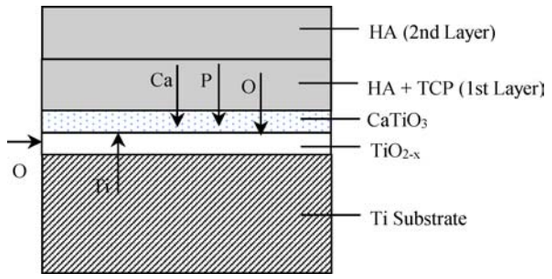

Figure 6 Schematic of the interfacial zone of HA-Ti coating system.

1. HA coating 2 (top layer): Free of decomposition and therefore bioactive and not resorbable.
2. HA coating 1 (under layer): Partial decomposition and therefore susceptible to *in vitro* dissolution if not completely covered by coating 2. While it would be difficult to ascertain whether complete coverage occurred (coating 1 over coating 2) via the physical analysis used in this study (SEM, XRD, EDS), *in vitro* or implantation studies with thermally sprayed HA and monolithic HA control specimens would be beneficial in this regard.
3. $CaTiO_3$ interfacial reaction region: This was located between HA coating 1 and the oxide layer. The presence of this layer was indicative of a strong chemical bond between the HA and the metal.
4. Oxide layer: This was negligible in the 316L stainless steel specimens but substantial in the Ti and Ti6Al4V specimens. The size of this layer is indicative of the oxidation resistance of the metal. Interestingly, previous interfacial strength studies by the authors have revealed that failure usually occurs within this zone and so it is therefore the weak link in the interface [12]. It is probable that the size of this zone cannot be reduced by using extremely low oxygen partial pressures (thoroughly gettered argon feed gas) since the HA itself is a source of oxygen.
5. Metallic substrate: As the temperature-tensile strength study established, the tensile strength of the metallic substrate was virtually unaffected by the densification of the HA at temperatures of 1000 °C or lower. Since the authors have established in a previous study, that 1000 °C is adequate for the attainment of significant HA-metal interfacial strength [12], the issue of degradation of metal strength is probably not a significant concern.

Acknowledgments

The assistance of Dr C.H. Kong with the electron microscopy is gratefully acknowledged.

References

1. J. C. KNOWLES, K. GROSS, C. C. BERNDT and W. BONFIELD, *Biomater.* **17** (1996) 639.
2. A. J. RUYS, C. C. SORRELL, A. BRANDWOOD and B. K. MILTHORPE, *J. Mater. Sci. Lett.* **14** (1995) 744.
3. C. CHAI and B. BEN-NISSAN, *Int. Ceram. Monogr.* **1** (1994) 66.
4. P. DUCHEYNE, S. RADIN, M. HEUGHEBAERT and J. C. HEUGHEBAERT, *Biomater.* **11** (1990) 244.

5. A. MILEV, G. S. K. KANNANGARA and B. BENNISSAN, *Mater. Lett.* **57** (2003) 1960.
6. R. CHIESA, E. SANDRINI, M. SANTIN, G. RONDELLI and A. CIGADA, *J. App. Biomater. & Biomechan.* **1** (2003) 91.
7. M. WEI, M. UCHIDA, H. KIM, T. KOKUBO and T. NAKAMURA, *Biomater.* **23** (2001) 167.
8. M. WEI, A. J. RUYS, B. K. MILTHORPE, C. C. SORRELL and J. H. EVANS, *J. Sol-Gel Sci. & Tech.* **21** (2001) 39.
9. P. DUCHEYNE, W. V. RAEMDONCK, J. C. HEUGHEBAERT and M. HEUGHEBAERT, *Biomater.* **7** (1986) 97.
10. A. J. RUYS, C. C. SORRELL, A. BRANDWOOD and B. K. MILTHORPE, *J. Mater. Sci. Lett.* **14** (1995) 744.
11. M. WEI, M. V. SWAIN, A. J. RUYS, B. K. MILTHORPE and C. C. SORRELL, *Mater. Eng.* **9** (1998) 19.
12. M. WEI, A. J. RUYS, M. V. SWAIN, S. H. KIM, B. K. MILTHORPE and C. C. SORRELL, *J. Mater. Sci. Mater. Med.* **10** (1999) 401.
13. M. WEI, M. V. SWAIN, A. J. RUYS, B. K. MILTHORPE and C. C. SORRELL, *Mater. Eng.* **9** (1998) 7.
14. C. S. KIM and P. DUCHEYNE, *Biomater.* **12** (1991) 461.
15. C. T. CHU and B. DUNN, *Appl. Phys. Lett.* **55** (1989) 492.
16. J. BREME, Y. ZHOU and L. GROH, *Biomater.* **16** (1995) 239.
17. J. B. PARK and R. S. LAKES, in "Biomaterials: An Introduction," 2nd edn. (Plenum Press, New York, 1992).
18. C. J. E. SMITH and A. N. HUGHES, *Eng. Med.* **7** (1966)158.
19. R. VAN NOORT, *J. Mater. Sci.* **22** (1987) 3801.
20. A. J. RUYS, K. A. ZEIGLER, O. C. STANDARD, A. BRANDWOOD, B. K. MILTHORPE and C. C. SORRELL, in Ceramics: Adding the Value, edited by M. J. Bannister (CSIRO, Melbourne, 1992) p. 605.
21. A. J. RUYS, K. A. ZEIGLER, B. K. MILTHORPE and C. C. SORRELL, in Ceramics: Adding the Value, edited by M. J. Bannister (CSIRO, Melbourne, 1992) p. 591.
22. A. J. RUYS, N. EHSANI, B. K. MILTHORPE and C. C. SORRELL, *J. Aust. Ceram. Soc.* **29** (1993) 65.
23. A. J. RUYS, A. BRANDWOOD, B. K. MILTHORPE, M. R. DICKSON, K. A. ZEIGLER and C. C. SORRELL, *J. Mater. Sci. Mater. Med.* **6** (1995) 297.
24. H. JI and P. M. MARQUIS, *Biomater.* **14** (1993) 64.
25. P. DUCHEYNE, P. D. BIANCO and C. KIM, *Biomater.* **13** (1992) 617.
26. K. A. ZEIGLER, A. J. RUYS and C. C. SORRELL, in Proceedings of the 3rd Australian Forum on Metal Matrix Composites, edited by S. Bandyopadhyay and A. G. Crosky (IMMA, Sydney, 1992) p. 175.
27. A. G. COCKBAIN, *Min. Mag.* **36** (1968) 654.
28. M. WEI, A. J. RUYS, B. K. MILTHORPE, A. BRANDWOOD and C. C. SORRELL, *Int. Ceram. Mono.* **2** (1998) 3.
29. I. ZHITOMIRSKY and L. GAL-OR, *J. Mater. Sci. Mater. Med.* **8** (1997) 213.
30. M. WEI, A. J. RUYS, B. K. MILTHORPE and C. C. SORRELL, *Mater. Lett.* (Submitted).
31. M. JARCHO, C. H. BOLEN, M. B. THOMAS, J. BOBICK, J. F. KAY and R. H. DOREMUS, *J. Mater. Sci.* **11** (1976) 2027.
32. B. F. YETER-DAL, V. GROSS and T. W. TURNEY, in Ceramics: Adding the Value, edited by M. J. Bannister (CSIRO, Melbourne, 1992) p. 617.
33. T. FUTAGAMI and T. OKAMOTO, *J. Ceram. Soc. Japan.* **95** (1987) 775.

Received 27 February
and accepted 12 August 2004